Optimization of Machining Parameters of Abrasive Jet Machining for Drilling Silica Glass

Atira Aziz[1] , Rahul Mittal[1]
[1]Universal Institute of Engineering & Technology, Lalru,Mohali

---

Abstract : *In addition to being used for machining tougher materials, Abrasive Jet Machining (AJM) may often be used for machining brittle materials. The energy is transferred at high-speed particles that are impinging on the surface of the work piece and material is separated through brittle fracturing and micro-cutting motion. The aim of this analysis was to maximize the results of the process parameters of abrasive jet machining for drilling at the production level of soda-lime silica glass. Experiments were accomplished in the indigenously built and constructed setup that was developed in the institute. In response portion, we followed a treatment response surface to analysis and chart the experiments. Various variables such as variance of input parameters induced differences in the material removal rate and the drilled hole duration. These models were built based on a mathematical analysis that consists of test-based or Q-methods and regression techniques. It was observed that the hole of the pipe decreased with the rise in the strain and decrease in the separation gap. By utilizing his response model more, we can now generate a dimensionless desirability function based on the Derringer desirability function method.*

1. INTRODUCTION

Technical studies and exploratory exercises confirming the value of the erosive action of hard materials have also led to developing the abrasive jet setting. Study on the particle impact of the mixture of smoke and dust on different types of substances [1] has been carried out. Prior to 1940, the mechanism of soil forming was not understood. Later experiments on special aero foils, inlet ducts, and diverse modes offered an appreciation of further molecular impact problems. Under various controlled environments, Wellinger and his co-researchers obtained erosion data, but failed to establish statistical correlations between the data and the material removal or physical properties of the material. The experimental experiments were distinctive, investigating distinct impingement angles. Their investigation found that the major determining variables in material reduction were mechanical characteristics, although there were other aspects that also played a role.

Wear is a system in which the processing of substance is attributable to the reaction of two surfaces. There are no general wear mechanism rules. Burwell has been leading a review of conceivable wear components [6]. When two surfaces were in touch, he examined the wear process, which was the loss of material. This analysis and several separate experiments have shown that abrasive wear has been of significant significance. Sliding of abrasives at first sight was considered by Moore [7], accentuating the variety of criteria that influence the abrasive wear of materials. Particle displacement relative to each other and rotation were illuminated when sliding around the wearing surface and three body abrasive wear tests were taken into account. This principle has considerable importance in AJM, for both rotation and slipping would be exposed to the numerous abrasive particles hitting a rock. Many scholars use the works of Rabinowicz and Mutis to shed some attention on the hypotheses of abrasive wear.

In 1960, Finnie [1] found that the ductile and brittle material removal process was often influenced by the predominant flow conditions during AJM. The problem of erosion was split into two main components, i.e. finding it to be a two-phase flow question and material removal measurement. For ductile products, material removal during AJM was predictable, with a variation in the path and velocity of the abrasive particles. It was very hard, though, to foresee the same in the case of fragile materials. The connection between material removal and controlling input parameters has been found for ductile materials, as seen in (Equation 1).

$$E = \frac{Cf(\theta)MU^n}{\sigma_{w(min)}} \quad ....(1)$$

Where 'E' is the amount of material removed;' M' is the density of abrasive particles;' C' and 'n' are constants;' U' is the velocity of the particles impacting,'σw (min)' is the target material's minimal flow stress and ' θ 'is the angle of impingement. In addition, Bitter[8] updated (1) by adding the definition of the minimum energy threshold and the efficient angle of impingement. The minimal threshold energy is the energy density of the particles at which brittle corrosion can not be accomplished. In addition, Neema and Pandey[9] suggested a mathematical model for the representation of MRR 'E' as seen in (2).

$$E = 8kNr^3U^{\frac{3}{2}}\frac{P_a}{2\sigma_y} \quad ....(2)$$

Where 'k' is a constant,' N' is the number of particles and 'U' is the abrasive velocity,' r' is the abrasive particle radius,'σy' is the working material yield stress, and' Pa 'is the abrasive particle pressure.

Evans[10] assessed that the expansion and penetration of the surface is marked by material removal and impact fracturing. Degradation of strength and corrosion of the workpiece was delegated. The heterogeneity of crater volume and energy depletion by various impact angles and velocity has been clarified effectively by Hutching [11]. The material erosion was based on two characteristics, first on the morphology of the particles and second on the target material. In order to evaluate the rebound speed for oblique effect, the model produced was successfully implemented.

Most analysis has been carried out on abrasive wear by Rabinowicz and Mutis [12], [13]. He conducted tests with lubricated surfaces of copper and nylon, which were in reasonable compliance with the essential abrasive size believed and weighed. Large troubling causes have been addressed, such as adhesive wear and abrasive removal while slipping. The relationships between wear rates and slipping period, abrasive grain size and strength of the material were calculated. During 2-body abrasion, it has been shown to be close to the prevalent ones. The effects of moisture and the abrasive stream rate were studied and when these two variables were monitored, great reproducibility was observed. The abrasive wear rate was observed to be 10 times lower during 3-body abrasion than during 2-body abrasion. The explanation was presumably because 90 percent of the typical abrasive grain was rolling and only 10 percent abraded the sliding surfaces between which it is located.

Erosive cutting of brittle materials has been examined by Sheldon and Finnie[14],[15]. Various experiments utilising angular silicon carbide pellets and steel shots have been done on fragile materials. It was discovered that due to Hertzion interaction pressures, erosion was induced. Their study was helpful in showing that, under certain limitations of abrasive particle size and speed, the materials acted as though they were ductile ones.

2. EXPERIMENTAL SETUP

The experimental rig for AJM was planned and produced in the workshop of the institute. In addition to the filter regulator (FR) unit, AJM adapters were often included in the house air compressor. The air distributor, abrasive feeder, mixing chamber, nozzle, operating storage mechanism and glass chamber are separate components installed during this function. The modelling operation was carried out using tools from AutoCAD 2016 and ANSYS 16.2. In compliance with the core composite architecture methodology, tests were carried out on indigenously built and assembled installations. Air is compressed at a pressure of about 5 to 8 bar and has been integrated into the FR unit. The 8 mm polyurethane (PU) pipe was used to establish contacts between the air compressor and the FR unit, and other connections were also used. The air was further supplied to the dealer by the FR machine. On the vertical stand which supplies two supplies, the distributor was fixed. The seller stocks the abrasive feeder chamber with one distribution and the mixing chamber with a second delivery. The job keeping mechanism provides the work piece with upward and downward movement and, when required, provides separate SOD. Fig. 1 illustrates the experimental configuration of AJM elements of the experimental configuration utilising modelling tools such as dealer, abrasive feeder chamber and abrasive mixing chamber. In order to build the nozzle for the outlet velocity of fluid flowing through it, the geometrical nozzle model was created using AutoCAD and then exported to the ANSYS work area.

Figure 1 Experimental set-up

3. DESIGN METHODOLOGY

Because of the low cost and ease of availability relative to the nozzle of sapphire steel, tungsten carbide nozzles were used for experimentation in the setup. SOD is stored from 0.5 mm and 1.5 mm throughout the machining process. Air is compressed at a pressure of about 5 to 8 bar and has been integrated into the Filter Regulator (FR) unit. The 8 mm PU pipe was used to establish the links between the air compressor and the FR unit and other connections were also used. Due to its outstanding formability, weldability and economic aspects, mild steel content has been used for the manufacture of abrasive feeder chamber, distributor and mixing chamber. A 5 mm thick sheet of mild steel was used for the manufacture of the dealer, abrasive feeder chamber and mixing chamber.

The tests were carried out on soda-lime silica glass with a density of 2.53 g/cm3. T he chemical composition of the content of the workpiece is given as: SiO_2= 70-75 percent, Na_2O= 12-16 percent, CaO= 6-9 percent, MgO= 3-4 percent and Al_2O_3= 2 percent. With a Vickers amount of about 2600, the tungsten carbide nozzle is extremely hard. The ultimate tensile strength is approximately 340 MPa; the ultimate compression strength is approximately 2.6 GPa and the Poisson ratio is 0.31. In two separate sizes, i.e. 325 and 400 mesh, abrasive particles of SiC were used. The glass sheet scale 75 x 75 x 5 mm3 was used as a working material for testing and the machining period for each experiment was set at 40 seconds.

Abrasive, carrier gas, abrasive jet, and nozzle were primarily concerned with the process parameters that influence the consistency of the product being processed by AJM. Pressure, Stand of Distance (SOD) and abrasive size were the most popular of these criteria, which were taken as three separate parameters for thorough investigations. Experiments have been performed in multiple input environments. MRR was calculated using the mechanism of weight loss.

Fig.2 displays standard plot of residuals for MRR. It shows that the errors are usually distributed when the residual points land near the straight line. The relation between the expected value and the real value is shown in Fig 3 . It means that the model matches with the values observed.

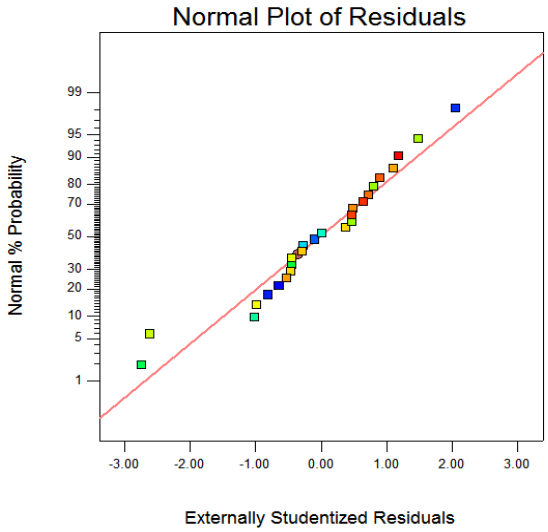

Figure 2 Normal probability plot of residuals for MRR

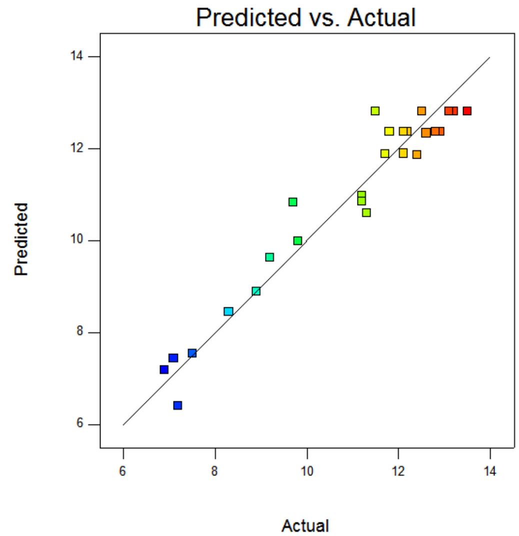

Figure 3 Plot of actual vs. predicted response of MRR

Fig. 4 displays the three-dimensional approximate reaction to the MRR in relation to the pressure and SOD geometry parameters for the 325 mesh abrasive scale. It shows that, with increasing pressure and SOD, the MRR first increases, reaches a certain value and then decreases. At 7.1 bar pressure and 1.1 mm SOD, the maximum MRR obtained from the plot is 1.297 mg/s. Impact of pressure and SOD on MRR for the 400 mesh abrasive scale, i.e. with an increase in strain, MRR first rises and then decreases, and SOD is seen in Fig. 5. This indicates that the maximal MRR was obtained at 7 bar pressure and 1 mm SOD, i.e. 1.365 mg/s. It also shows that, with increasing strain and SOD, the MRR first increases, reaches a certain value and then decreases.

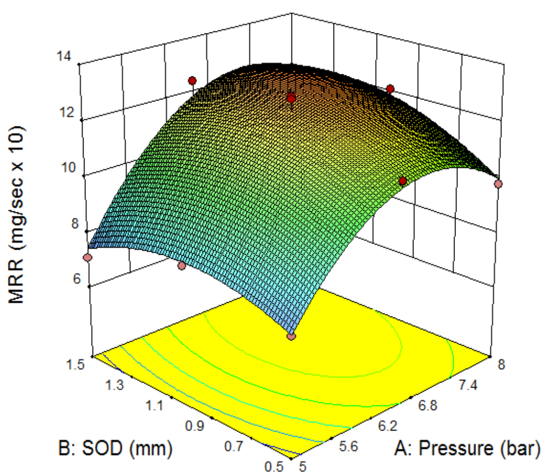

Figure 4 Effect of pressure and SOD on MRR for abrasive size of 325 mesh

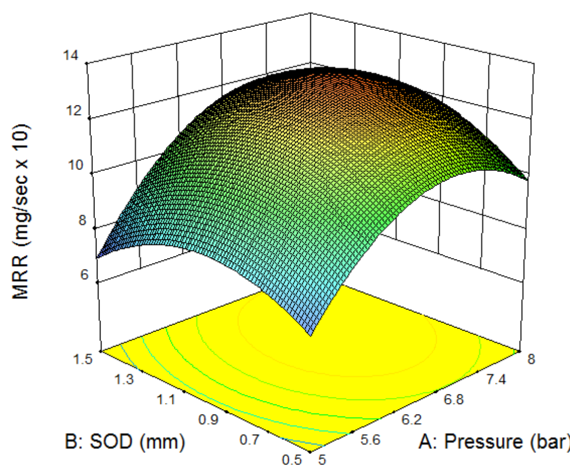

Figure 5 Effect of pressure and SOD on MRR for abrasive size of 400 mesh

Residuals of normal probability plots for DH are shown in Fig. 6. It shows that the errors are usually distributed when the residual points land near the straight line. The distinction between the expected value and the real value is shown in Fig.7. The regression model was shown to suit with the data from the input.

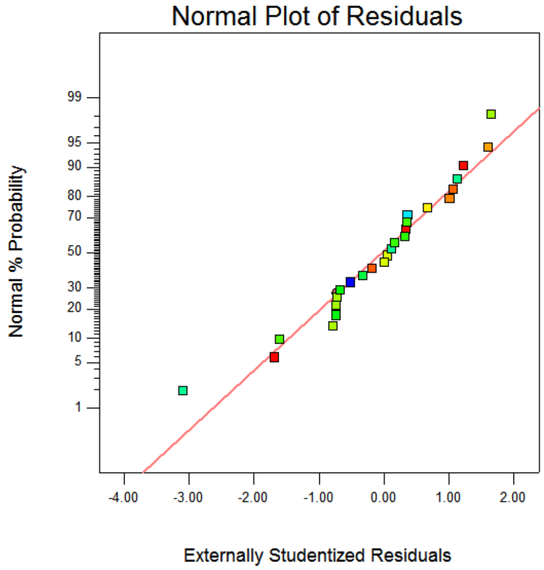

Figure 6 Normal probability plot residuals for DH

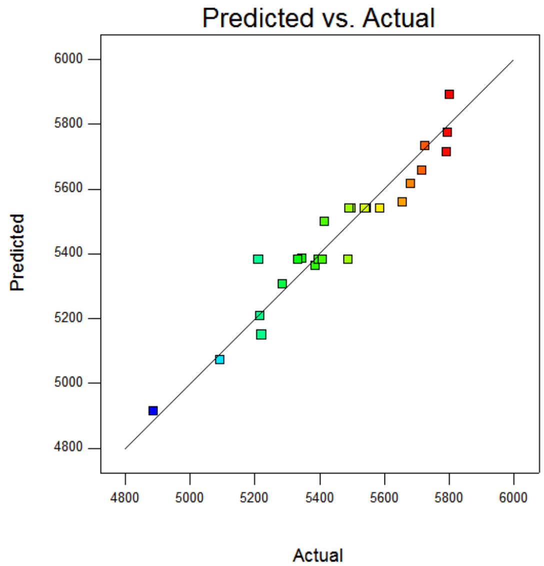

Figure 7 Plot of actual vs. predicted response of DH

Fig. 8 displays the approximate reaction to the DH in relation to the pressure geometry parameters and the SOD for the 325 mesh abrasive scale. It indicates that with an increase in pressure, the DH decreases and rises with an increase in SOD. At 8 bar pressure and 0.5 mm SOD, the minimum DH obtained was 5092.63 µm. For an abrasive scale of 400 mesh, the effect of pressure and abrasive size on DH is shown in Fig. 9. It indicates that 4886.94 µm is the minimum DH, which was obtained at 0.5 mm SOD and 8 bar pressure. It is found that by rising pressure and decreasing SOD, DH can be decreased.

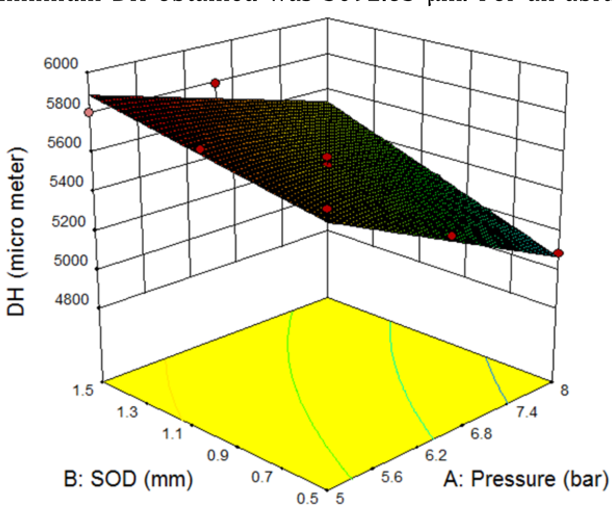

Figure 8 Effect of pressure and SOD on DH for abrasive size of 325 mesh

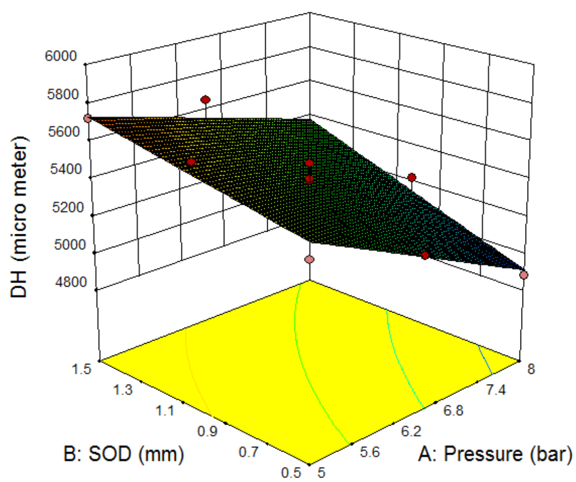

Figure 9 Effect of pressure and SOD on DH for abrasive size of 400 mesh

4. Result

There were two goals in this study, respectively. MRR maximisation and DH minimization. Throughout some design space, these two goals were in conflict with each other. Therefore, by using the method of Derringer and Suich [16], the two objectives were mixed together to create a single goal called the overall desirability function. The multivariate optimization problem has now been translated into a univariate one. For optimum parameter configuration for pressure, SOD and abrasive mesh size as 7,729 bar, 0,847 mm, 400 mesh, respectively, the optimal value of desirability was found to be 0.724. The optimum point relative to the abrasive mesh size 400 was found to yield better MRR and DH responses than its counterparts based on the 325 mesh. Confirmation tests were then carried out by taking an abrasive mesh scale of 400.

To verify the feasibility of the technically expected optimal performance, validation tests were needed to be carried out. Two experiments were conducted at optimum AJM conditions for validation purposes, and the average response of the two experiments was shown in Table 1.

Table 1 Results of confirmation experiments

Machining conditions			MRR (mg/sec)		DH (µm)	
Pressure	SOD	Abrasive size	Exp.	Predicted	Exp.	Predicted
7.729	0.847	400	1.1463	1.2393	5013.65	5123.693

Experimental and expected values for both MRR and DH are shown to be very similar to each other, indicating that these optimum settings can be used for soda-lime silica glass drilling based on AJM.

5. CONCLUSIONS

In order to achieve an optimum setting of process parameters for the indigenously built and produced experimental set-up, response surface methodology was carried out. This creates maximum MRR and desired DH via the drilling process on the silica glass of soda-lime. Polynomial calculations concerning the variance of MRR and DH in terms of pressure, SOD and abrasive mesh size within the defined range were driven by response surface methodology. Independent criteria, i.e. strain, influence both MRR and DH, such as SOD and abrasive scale. It has been found that with a rise in pressure and SOD, the MRR first rises, reaches a certain value and then decreases. In addition, in contrast to 325 mesh scale, MRR was more than 400 mesh size. It has been noticed that by rising strain and decreasing SOD, DH can be decreased. Less DH is also produced with a size of 400 mesh than 325 mesh. The cumulative effect obtained was 1.2393 mg/s and 5123.693 µm at 7.729 bar pressure, 0.847 mm SOD and 400 mesh scale of abrasive particles, i.e. the mean MRR and minimum DH. The validation experiments have shown that the MRR and DH experimental and expected values are similar. And then it demonstrates the outstanding machinability of the experimental conclusions.

REFERENCES

[1] I. Finnie, “Erosion of surfaces by solid particles,” Wear, vol. 3, no. 2. pp. 87–103, 1960.

[2] K. Wellinger and H. C. Brockstedt, “Versuche zur ermittlung des verschleisswiderstardes von werkotoffen fur blasversatzzohr sowie des einflusses der rohrver lengung bei blasversatzanlangen,” Gluckauf, vol. 78, p. 130, 1942.

[3] K. Wellinger and H. C. Brockstedt, “Ermittlung des verschleisswiderstandes von werkotoffen fur blasversatzrohe,” Stahl Eisen, vol. 62, p. 635, 1942.

[4] K. Wellinger, “Sandstrahlverschleiss an metallen,” Metallkunde, vol. 40, p. 361, 1949.

[5] K. Wellinger and H. Uetz, “Gleitverschleiss spulverschleiss strahlverschleiss unter der wirkung von korningen stoffen,” VDI Forschungsh., p. 449, 1955.

[6] J. T. Burwell, “Survey of possible wear mechanism,” Wear, vol. 1, pp. 119–141, 1957.

[7] M. A. Moore, “A review of two-body abrasive wear,” Wear, vol. 27, no. 1, pp. 1–17, 1974.

[8] J. G. A. Bitter, “A study of erosion phenomena,” Wear, vol. 6, no. 3. pp. 169–190, 1963.

[9] M. L. Neema and P. C. Pandey, “Erosion of glass when acted upon by an abrasive jet,” Proc. Int. Conf. Wear Mater., pp. 387–392, 1977.

[10] A. G. Evans, M. E. Gulden, and M. Rosenblatt, “Impact damage in brittle materials in the elastic-plastic response regime,” Proceedings of the Royal Society A: Mathematical, Physical and Engineering Sciences, vol. 361, no. 1706. pp. 343–365, 1978.

[11] I. M. Hutchings and D. G. R. N.H. Macmillan, “Further studies of the oblique impact of a hard sphere against a ductile solid,” Int. J. Mech. Sci., vol. 23, no. 11, pp. 639–646, 1981.

[12] E. Rabinowicz and A. Mutis, “Effect of abrasive particle size on wear,” Wear, vol. 8, no. 5, pp. 381–390, 1965.

[13] E. Rabinowicz, L. A. Dunn, and P. G. Russell, “A study of abrasive wear under three-body conditions,” Wear, vol. 4, no. 5, pp. 345–355, 1961.

[14] G. L. Sheldon and I. Finnie, “The mechanism of material removal in the erosive cutting of brittle materials,” J. Eng. Ind., vol. 88, no. 4, p. 393, 1966.

[15] G. L. Sheldon and I. Finnie, “On the ductile behavior of nominally brittle materials during erosive cutting,” J. Eng. Ind., vol. 88, no. 4, p. 387, 1966.

[16] G. Derringer and R. Suich, “Simultaneous-Optimization of Several Response Variables,” J. Qual. Technol., vol. 12, no. 4, pp. 214–219, 1980.